



**Optical Detection of Alcohols with a Cu(I)HETPHEN Complex  
by Reversible Aldehyde to Hemiacetal Conversion**

Journal:	<i>Analyst</i>
Manuscript ID	AN-COM-06-2023-001005.R1
Article Type:	Communication
Date Submitted by the Author:	07-Aug-2023
Complete List of Authors:	Wang, Lei; University of Shanghai for Science and Technology, School of Materials and Chemistry Xie, Zhulin ; Argonne National Laboratory, Li, Xin; University of Shanghai for Science and Technology Lynch, Vincent; University of Texas at Austin, Chemistry Mulfort, Karen; Argonne National Laboratory, Chemical Sciences and Engineering Division

## COMMUNICATION

## Optical Detection of Alcohols with a Cu(I)HETPHEN Complex by Reversible Aldehyde to Hemiacetal Conversion

Lei Wang,<sup>\*a,b</sup> Zhu-Lin Xie,<sup>b</sup> Xin Li,<sup>a</sup> Vincent M. Lynch,<sup>c</sup> and Karen L. Mulfort<sup>\*b</sup>

Received 00th January 20xx,

Accepted 00th January 20xx

DOI: 10.1039/x0xx00000x

**A heteroleptic copper(I) bis(phenanthroline) complex with aldehyde groups on 4,7 positions of the phenanthroline ligand were synthesized. The complex is responsive to alcohol, resulting in a distinct colour change caused by the facile reaction of the aldehyde group with alcohol, forming a hemiacetal product. The aldehyde species can be regenerated after heating the intermediate at 80°C for 10 minutes, demonstrating the reusability of the complex for alcohol detection. This work presents a new strategy of applying transition metal complexes for small molecule sensing by installing functional groups in the secondary coordination sphere that reversibly react with analytes.**

Short-chain alcohols, such as methanol, ethanol and propanol, are commonly used in recreation, medical field, and industrial processes. However, the residue of such volatile chemicals may pose serious health concerns, including fetal alcohol spectrum disorders, various types of cancer, cardiovascular disease, liver cirrhosis, due to their toxic and carcinogenic nature.<sup>[1]</sup> Furthermore, many organic reactions that involve alcohols require continuous monitoring of alcohols to prevent side reactions.<sup>[2]</sup> Therefore, there is a need for inexpensive and convenient methods to detect alcohols.

Despite the availability of numerous technologies and devices for alcohol detection,<sup>[3]</sup> many of them operate by a complicated mechanism and indirectly respond to alcohol analytes, making alcohol detection inconvenient. For example, most sensors composed of nanomaterials, such as TiO<sub>2</sub> nanotubes,<sup>[4]</sup> hexagonal ZnCo<sub>2</sub>O<sub>4</sub> grown on Ni foam,<sup>[5]</sup> graphene and graphene oxide (GO),<sup>[6]</sup> and metal-organic frameworks

(MOFs),<sup>[7]</sup> function via physical interactions with analytes based on their different shapes and pore sizes. These sensors are coupled to a transducer which converts the responses into measurable electrochemical or optical signals and then transmitted to processing systems. Hence, these devices require sophisticated design and incorporation of multiple components<sup>[8]</sup> and therefore developing a simple direct method to monitor liquid alcohol by a colour change, similar to pH indicators, has strong technological potential.

Transition metal complexes have demonstrated structural diversity and tunability of electronic structures, leading to various optical and electrochemical properties. As a result, they have been utilized in different fields, such as catalysis, energy conversion, magnetization, and sensing. Among them, copper(I)diimine complexes have drawn special attention because of their promising photochemical properties and potential application as photosensitizers in photocatalysis.<sup>[9]</sup> In our group, we have systematically studied the photophysics of various homonuclear Cu(I)diimine complexes<sup>[9]</sup> and investigated photo-induced directional charge transfer of Cu(I) chromophores in donor-acceptor complexes<sup>[10]</sup> and bimetallic Cu/Ru/Os assemblies.<sup>[11]</sup> Recently, we discovered that the optical and redox properties of Cu(I)diimine complexes can be modulated and controlled by changing the electron-donating or -withdrawing ability of the substituents on the 4,7 positions of the phenanthroline ligand<sup>[12]</sup>. In this work, as the Cu(I)diimine complexes were functionalized with stronger electron-withdrawing groups, the MLCT band was red-shifted up to 30 nm from the baseline R = H complex. This demonstrates the impact of the ligand substituent electronic effects in the secondary coordination environment on the photophysical properties of the Cu(I) complexes.

Based on this discovery, we herein expand the application of the Cu(I)diimine complexes to alcohol detection by the design and synthesis of a unique Cu(I) complex (**Cu-4,7-CHO**, Chart 1) featuring an aldehyde group on the 4,7 positions of the phenanthroline ligand. We observe that the aldehyde group

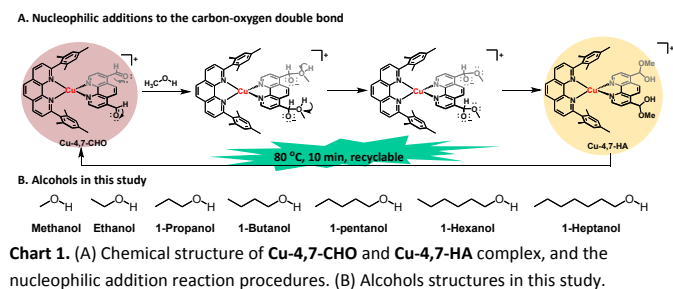
<sup>a</sup> School of Materials and Chemistry, University of Shanghai for Science and Technology, Shanghai 200093, P. R. China.

<sup>b</sup> Division of Chemical Sciences and Engineering, Argonne National Laboratory, Lemont, IL 60439.

<sup>c</sup> Department of Chemistry, University of Texas Austin, Austin, TX, 78712.

\* Corresponding author: leiwang@usst.edu.cn, mulfort@anl.gov.

Electronic Supplementary Information (ESI) available: [details of any supplementary information available should be included here]. See DOI: 10.1039/x0xx00000x



reacts with short-chain alcohols to yield a hemiacetal group which shifts the electronic effect of the 4,7-substituents from electron-withdrawing to electron-donating. The change in the electronic properties results in clear distinctions in the complex's colour and spectroscopic signatures, allowing for straightforward detection of medium concentrated alcohol. The reversibility of this reaction is well established in the literature<sup>[13]</sup>, and confirmed here using **Cu-4,7-CHO**, suggesting that the complex could be a potential candidate for the development of reusable indicators for alcohol detection.

During the <sup>1</sup>H NMR characterization of **Cu-4,7-CHO**, a sharp signal at ~10.7 ppm was observed in deuterated chloroform, acetone, acetonitrile and DMSO which we assign to the aldehyde proton (-CHO), and this resonance shifts slightly downfield with more polar media as reported before<sup>[14]</sup> (Fig. S10). However, in deuterated methanol there is no peak between 10-11 ppm and instead a singlet shifts substantially up-field at 6.19 ppm (Fig. 1A). In a similar situation, <sup>13</sup>C NMR shows a 193.3 ppm in acetone-*d*<sub>3</sub> (Fig. S5) and while a 159.8 ppm in methanol-*d*<sub>4</sub> (Fig. S7).

The shifts in the NMR spectra were puzzling until we considered conversion of the aldehyde group to the hemiacetal (-CH(OH)OCH<sub>3</sub>). Single crystals of **Cu-4,7-CHO** were grown by slow evaporation from dichloromethane and diethyl ether and

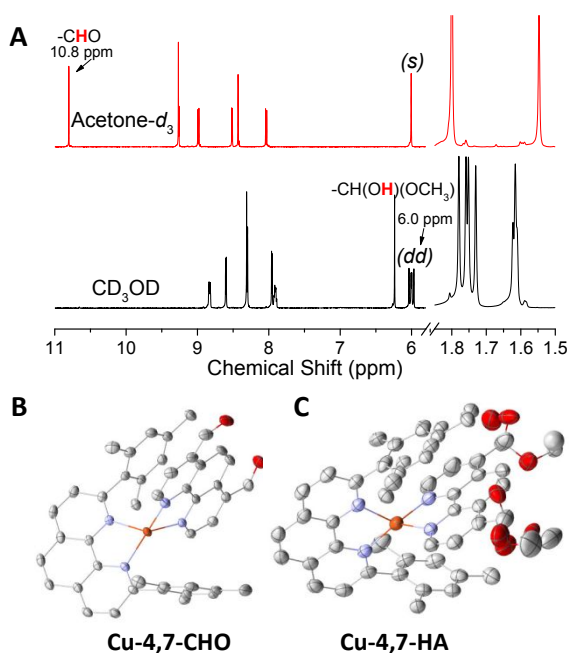


**Fig. 1** (A) <sup>1</sup>H NMR spectrum and (B-C) Single-crystal structures of complexes **Cu-4,7-CHO** and **Cu-4,7-HA**.

confirms the heteroleptic coordination geometry of the complex<sup>[12]</sup>. We unambiguously confirmed formation of the hemiacetal functionalized complex, **Cu-4,7-HA**, by analysis of single crystals grown by slow evaporation from methanol and diethyl ether (Fig. S17-S18, and Table S1-S2). Both **Cu-4,7-CHO** and **Cu-4,7-HA** show typical "pac-man" geometry of CuHETPHEN complex as we reported before. It reveals that **Cu-4,7-HA** crystal structure shows a smaller distortion from tetrahedral geometry (*s*<sub>4</sub> = 0.692) than **Cu-4,7-CHO** (*s*<sub>4</sub> = 0.680), which highly related with the steric effect of larger hemiacetal group.

With conclusive evidence of hemiacetal formation to yield **Cu-4,7-HA**, we can now confidently assign the singlet at 6.19 ppm to the original aldehyde proton, now α- to the -CH- group of the hemiacetal, which appears at a resonance typical for similar functional groups.<sup>[15]</sup> The splitting of the mesityl protons from singlets to doublets is the result of 1) the hemiacetal **Cu-4,7-HA** has two stereocenters and therefore two pair of diastereomers can be formed, with the -CH<sub>3</sub> groups in mesityl becoming not equivalent; 2) the close interactions between the aromatic and aliphatic protons of the mesityl group with the methyl group of the hemiacetal. This close interaction is also observed in the crystal structure of **Cu-4,7-HA**, as shown in Fig. 1C. Formation of the hemiacetal is also confirmed by mass spectrometry as the *m/z* detected for **Cu-4,7-CHO** in acetonitrile is what we expect for the aldehyde form (calcd 715.21; found 715.42) but increases in methanol to what is expected for **Cu-4,7-HA** (calcd 779.26; found 779.50, Fig. S11). The 2D <sup>1</sup>H-<sup>1</sup>H COSY spectrum is also used to confirm the connectivity between neighbouring protons in the complex, as shown in Fig. S12-S13. The strong correlation between H1 and H2 further prove the formation of hemiacetal in methanol. We compared the NMR spectrum of **Cu-4,7-CHO** in deuterated acetone with adding 4% and 20% (by volume) deuterated methanol in 1 mM **Cu-4,7-CHO** acetone solution. Fig. S14 demonstrates the up-field shift of the

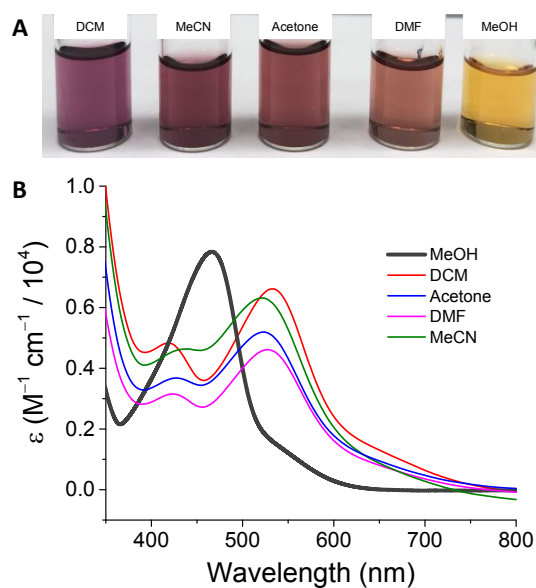
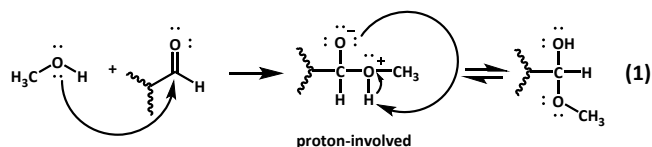


**Fig. 2** (A) Photograph of 500 μM **Cu-4,7-CHO** in indicated solvents. (B) UV-visible absorption spectra of 500 μM **Cu-4,7-CHO** in various solvents compared with **Cu-4,7-HA** in methanol.

original aldehyde peak and the splitting of the mesityl protons as the aldehyde groups are gradually attacked by methanol. The reactions of aldehyde and methanol also happened for 1,10-phenanthroline-4,7-dicarbaldehyde ligand, as confirmed by the NMR differences in methanol and dimethyl sulfoxide, as shown in Fig. S15-S16.

The UV-Vis absorption spectra of **Cu-4,7-CHO** were measured in different solvents at room temperature and their MLCT wavelength and extinction coefficients ( $\epsilon$ ) are summarized in Table S3. The observed UV-vis spectrum in methanol peaked at 467 nm (MLCT) is very different from other solvents. As proven by single crystal structures, this big difference of UV-vis is attributed to the reaction of the -CHO group with methanol to form a hemiacetal group via a nucleophilic addition mechanism according to Equation (1)<sup>[16]</sup>.



Changes in spectral absorption are also accompanied by a distinctive colour change of complex **Cu-4,7-HA** in methanol (orange) and complex **Cu-4,7-CHO** in other solvents (reddish) at the same concentration (500  $\mu$ M), as shown in Fig. 2. The formation of hemiacetal group was further proved by the calculated electronic spectra of **Cu-4,7-CHO** in both dichloromethane and methanol using TD-DFT analysis<sup>[17]</sup>. We found that the theoretical spectra of **Cu-4,7-CHO** well with the experimental spectrum in dichloromethane, and we did not observe any significant difference between the results in dichloromethane and methanol (Fig. S19). This suggests that solvents have minor impact on the spectra. However, when the calculation was performed for **Cu-4,7-HA** then the theoretical and experimental results fit perfectly (Fig. S20). To explain this, natural transition orbitals (NTOs) based on the TD-DFT calculation were generated to visualize the dominant transitions.

It's worth noting that distinguished from other CuHETPHEN complexes with  $\sim$ 465 nm as its characteristic MLCT absorption peak<sup>[9]</sup>, **Cu-4,7-CHO** complex shows an unusual peak-splitting behaviour in most of the studied solvents, in which the MLCT bands peaked at 422 nm and 530 nm. Splitting of the MLCT manifold has been observed previously for heteroleptic ruthenium complexes as a result of the lowest energy metal-to-ligand transitions occurring to multiple  $\pi^*$  acceptor ligands of similar energy levels<sup>[18]</sup>. This has also been previously reported for CuHETPHEN complexes with biquinoline-based ligands and with 4,7-dicarboxylic acid-1,10-phenanthroline as the secondary ligand<sup>[19]</sup>.

The difference in the absorption spectra of **Cu-4,7-CHO** and **Cu-4,7-HA** can be attributed to the energy of the transitions to two different ligands become similar in hemiacetal complex, showing only one peak at the MLCT band of hemiacetal (Fig. S21).

In fact, this sensitivity to alcohols was also found for Cu-2,9-CHO complex, shown in Fig. S22, proving the versatile strategy of using aldehyde-containing copper complexes as alcohol

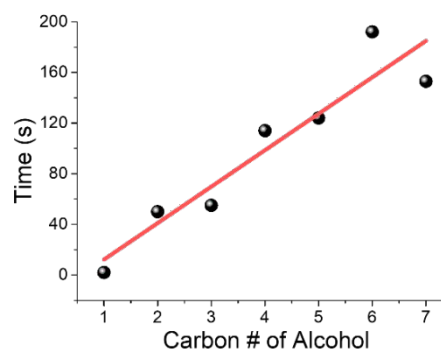


Fig. 3 Plot of "reacting time" versus the length of alcohol.

indicator. However, the absorption of Cu-2,9-CHO complex displays a blue-shift characteristic in comparison to **Cu-4,7-CHO** complex, and the space between the two peaks in bimodal spectra of Cu-2,9-CHO ( $\Delta\lambda = 80$  nm) is smaller than that of **Cu-4,7-CHO** ( $\Delta\lambda = 97$  nm). This result is consistent with the TD-DFT calculation results (Fig. S22). The NTOs (Fig. S24) clearly showed that the 4,7-positions have larger spin density than 2,9-position, hence putting substituents on 4,7-position have an outsized effect on Cu(I) complex properties.

Given the facile reactivity of **Cu-4,7-CHO** in the presence of alcohols and unique optical signatures, we hypothesized that **Cu-4,7-CHO** may be of interest in detecting alcohols. Hence, the influence of various alcohols on the optical properties were systematically investigated. In order to explore the reaction kinetics, a large excess of particular alcohols was added to a solution of **Cu-4,7-CHO** in acetone (mole ratio of alcohol to complex = 1400) and monitored the absorbance spectrum. To facilitate quantitative comparison of sensitivity to different alcohols, we defined a "reacting time",  $\tau$ , as the cross-point time of the absorption-time plot at 469 nm and at 524 nm. By monitoring the spectral changes with time (Fig. S25), we found that the MLCT band immediately ( $\tau < 1$  s) transforms from bimodal to unimodal on addition of methanol, while other alcohols show observable "reacting time". There is a linear relationship between  $\tau$  and the length of the alcohol chain (Fig. 3), presumably due to the stronger steric effects and larger electron cloud density of the alcohol with longer chain than the alcohols with shorter chain, i.e. the nucleophilicity of alcohol is decreased in the presence of large-sized aliphatic chain. This observation is consistent with previous report that the reactivity decreased with increasing the length of alcohols<sup>[20]</sup>. As shown in Fig S26, the plot of  $\log(k/k(\text{CH}_3))$  versus polar substituent ( $\sigma^*$ ) or steric substituent constant ( $E_s$ ) follows the Taft equation. In addition, the viscosity and diffusion coefficient differences would also play a minor role on the initial reactivity (Table S4), we assume these all impact the real reacting time. This linear sensitivity to alcohols demonstrates its ability of being alcohol indicator.

To further understand the reactivity of **Cu-4,7-CHO**, spectrophotometric titrations were performed for complex in acetone by successive additions of methanol and methanol- $d_4$  while monitoring the spectra between 350 nm and 800 nm. Increasing the content of titrant in solution resulted in a blue shift of MLCT and the MLCT band gradually changed from bimodal to unimodal. As shown in Fig. S27, to reduce the

absorption at 524 nm from 100% to 50%, more methanol (3.3 M) is required than deuterated methanol (1.55 M) because of the potential kinetic isotope effect in the proton-involved step. In the context of proton-involved reactions, Stern-Volmer expression is often applied to calculate the H-bonding equilibrium constant,  $K_{HB}^{[21]}$ . For the purposes of comparing the  $K_{HB}$  in methanol and deuterated methanol, here, we derived a "pseudo-Stern-Volmer" equation (2):

$$\frac{A_0}{A_{obs@524\text{ nm}}} - 1 = \frac{c[alcohol]}{1 + K_{HB}[alcohol]} \quad (2)$$

where  $A_0$  is the absorption in pure acetone,  $A_{obs@525nm}$  is the absorption with adding different amount of titrant,  $K_{HB}$  is the equilibrium constant for H-bonding between aldehyde and alcohol, [alcohol] is the concentration of added methanol and  $c$  is a rate constant. The plots of points and fitted traces are presented in Fig. S27 and the calculated values of  $K_{HB}$  in methanol and deuterated methanol are 0.6387 and 0.3553 respectively, resulting in a  $K_{HB(H)}/K_{HB(D)}$  value of 1.80. The KIE of  $\sim 2$  is consistent with the proton involvement presumed in the aldehyde to hemiacetal conversion.

To demonstrate the recyclability for alcohol detection, **Cu-4,7-CHO** was dissolved in methanol and then dried at 80°C for 10 min. The obtained product was re-dissolved in dichloromethane and the bimodal spectra re-appeared, as shown in Fig. S28. The reversible bimodal-to-unimodal spectral behaviour of **Cu-4,7-CHO** illustrates the advantageous character of **Cu-4,7-CHO** as alcohol indicator. Many developed indicators such as pH-test paper are disposable and cannot be reused after detecting the target species. However, **Cu-CHO** reported herein is completely recyclable and has the potential of long-lasting reusability.

Copper complexes containing aldehyde group present an interesting opportunity to monitor and detect alcohols. Here we reported that  $[\text{Cu}(\text{mesphen})(4,7\text{-CHO-phen})]^+$  shows solvent-responsive behaviour and presents an unusual colour change in alcohol compared with other solvents. Both NMR and UV-Vis spectra validate the formation of hemiacetal and kinetic behaviours in responding to adding alcohols. More interestingly, this **Cu-4,7-CHO** complex presents different behaviour as a function of alcohol chain length. Considering the fact that many transition metal complexes can cause colour change by tuning the ligands or even just the substituents, we believe that this work should shed light on developing more selective indicators based on transition metals complexes.

This work is supported by the Division of Chemical Sciences, Geosciences, and Biosciences, Office of Basic Energy Sciences of the U.S. Department of Energy through Contract No. DE-AC02-06CH11357, and the National Natural Science Foundation of China (22205144). We gratefully acknowledge the computing resources provided on Bebop, a high-performance computing cluster operated by the Laboratory Computing Resource Center at Argonne National Laboratory.

## Author Contributions

Lei Wang contributes to synthesis, conceptualization, data curation, formal analysis, investigation, funding acquisition, writing – original draft and funding acquisition; Zhu-Lin Xie contributes to data curation (DFT calculations), formal analysis and writing – review & editing; Xin Li contributes to partial UV-vis measurement; Vincent M. Lynch contributes to single crystal measurement and data collection; Karen L. Mulfort contributes to conceptualization, validation, supervision, funding acquisition, and Writing – review & editing. All authors have given approval to the final version of the manuscript.

## Conflicts of interest

There are no conflicts to declare.

## Notes and references

‡ CCDC 2226033 and CCDC 2226034 contain the supplementary crystallographic data for this paper. These data can be obtained free of charge from The Cambridge Crystallographic Data Centre via [www.ccdc.cam.ac.uk/structures](http://www.ccdc.cam.ac.uk/structures).

- [1] A. S. Campbell, J. Kim and J. J. C. o. i. e. Wang, *2018*, *10*, 126-135.
- [2] Y. Wang, Z. Huang and Z. J. N. C. Huang, *2019*, *2*, 529-536.
- [3] M. P. Polat, D. Akyüz, H. Y. Yenilmez, A. Koca, A. Altındal and Z. A. J. D. T. Bayir, *2019*, *48*, 9194-9204.
- [4] P. Zhao, Y. Tang, J. Mao, Y. Chen, H. Song, J. Wang, Y. Song, Y. Liang and X. Zhang, *Journal of Alloys and Compounds* **2016**, *674*, 252-258.
- [5] Z. Yin, Z. Sun, J. Wu, R. Liu, S. Zhang, Y. Qian and Y. Min, *Applied Surface Science* **2018**, *457*, 1103-1109.
- [6] X. Huang, Z. Yin, S. Wu, X. Qi, Q. He, Q. Zhang, Q. Yan, F. Boey and H. Zhang, *Small* **2011**, *7*, 1876-1902.
- [7] W. P. Lustig, S. Mukherjee, N. D. Rudd, A. V. Desai, J. Li and S. K. Ghosh, *Chemical Society Reviews* **2017**, *46*, 3242-3285.
- [8] R. Boroujerdi, A. Abdelkader and R. Paul, *Nano-Micro Letters* **2020**, *12*, 1-33.
- [9] a) L. Kohler, R. G. Hadt, D. Hayes, L. X. Chen and K. L. Mulfort, *Dalton Trans.* **2017**, *46*, 13088-13100; b) L. Kohler, D. Hayes, J. Hong, T. J. Carter, M. L. Shelby, K. A. Fransted, L. X. Chen and K. L. Mulfort, *Dalton Trans.* **2016**, *45*, 9871-9883.
- [10] M. S. Eberhart, B. T. Phelan, J. Niklas, E. A. Sprague-Klein, D. M. Kaphan, D. J. Gosztola, L. X. Chen, D. M. Tiede, O. G. Poluektov and K. L. Mulfort, *Chemical Communications* **2020**, *56*, 12130-12133.
- [11] a) Z. L. Xie, X. Liu, A. J. Valentine, V. M. Lynch, D. M. Tiede, X. Li and K. L. Mulfort, *Angewandte Chemie International Edition* **2022**, *61*, e202111764; b) M. W. Mara, B. T. Phelan, Z.-L. Xie, T. W. Kim, D. J. Hsu, X. Liu, A. J. Valentine, P. Kim, X. Li and S.-i. Adachi, *Chemical Science* **2022**.
- [12] Z.-L. X. Lei Wang, Brian T. Phelan, Vincent M. Lynch, Lin X. Chen, Karen L. Mulfort, *Angewandte Chemie International Edition* **submitted**.
- [13] a) F. McKenna, H. Tartar and E. J. J. o. t. A. C. S. Lingafelter, **1953**, *75*, 604-607; b) J. J. A. C. Forrester, **1960**, *32*, 1668-1670.
- [14] a) H. Christenson, S. E. Friberg and D. W. J. T. J. o. P. C. Larsen, **1980**, *84*, 3633-3638; b) R. Streck, A. J. J. S. A. P. A. M. Barnes and B. Spectroscopy, **1999**, *55*, 1049-1057.
- [15] a) D. Boucher, J. Madsen, N. Caussé, N. Pèbère, V. Ladmiral and C. J. R. Negrell, **2020**, *1*, 89-101; b) B. Buchs, W. Fieber, D. Drahoňovský, J. M. Lehn, A. J. C. Herrmann and biodiversity, **2012**, *9*, 689-701.
- [16] C. D. Hurd, *Journal of Chemical Education* **1966**, *43*, 527.
- [17] a) H. S. Yu, S. L. Li and D. G. Truhlar, *The Journal of chemical physics* **2016**, *145*, 130901; b) R. L. Martin, *The Journal of chemical physics* **2003**, *118*, 4775-4777.
- [18] D. L. Ashford, C. R. Glasson, M. R. Norris, J. J. Concepcion, S. Keinan, M. K. Brennaman, J. L. Templeton and T. J. J. i. c. Meyer, **2014**, *53*, 5637-5646.
- [19] a) M. S. Eberhart, B. T. Phelan, J. Niklas, E. A. Sprague-Klein, D. M. Kaphan, D. J. Gosztola, L. X. Chen, D. M. Tiede, O. G. Poluektov and K. L. Mulfort, *Chem. Commun.* **2020**, *56*, 12130-12133; b) M. G. Fraser, H. van der Salm, S. A. Cameron, A. G. Blackman and K. C. Gordon, *Inorg. Chem.* **2013**, *52*, 2980-2992.
- [20] A. Osatiashiani, L. J. Durdell, J. C. Manayil, A. F. Lee and K. J. G. C. Wilson, **2016**, *18*, 5529-5535.
- [21] a) S. V. Lymar, G. F. Manbeck and D. E. Polyansky, *Chemical Communications* **2019**, *55*, 5870-5873; b) C. Turro, S. H. Bossmann, Y. Jenkins, J. K. Barton and N. J. Turro, *Journal of the American Chemical Society* **1995**, *117*, 9026-9032; c) L. Wang, D. W. Shaffer, G. F. Manbeck, D. E. Polyansky and J. J. Concepcion, *ACS Catalysis* **2019**, *10*, 580-585.